Evaluation of the Fluid-Structure Interaction of a Hydrokinetic Turbine Blade by Computational Fluid Dynamics and Finite Element Analysis

Juan Diego Betancur G*[1], Juan Gonzalo Ardila M[2], Edwin Lenin Chica A[3],
Jonathan Andrés Graciano U[1], Sebastián Velez García[1]

[1]Departmet of Mechatronics and Electromechanical, Instituto Tecnológico Metropolitano, Medellín, Colombia.

[2]Department of Agronomy, Universidad Surcolombiana, Neiva, Colombia.

[3]Department of Mechanical Engineering, Universidad de Antioquia, Medellín, Colombia.

ORCIDs: 0000-0002-3546-8311 (Juan Diego), 0000-0003-4461-7195 (Juan Gonzalo), 0000-0002-5043-6414 (Edwin Chica)

0000-0002-3950-4586 (Jonathan Andres), 0000-0001-7571-4049 (Sebastián Vélez)

Abstract

Hydrokinetic turbines (THK) convert kinetic energy from rivers, tidal currents, and waves into mechanical work that then, can be converted to electrical energy. An important aspect of hydrokinetic technology is the relationship between design simplicity, reliability, and system costs because represent significant differences compared to other renewable technologies. The blades of hydrokinetic energy converters in the current are very important since have a higher impact on the turbine performance and they are the components more expensive of the turbine. Aerodynamics profile shapes interact with the blades and it generated stresses and cause problems that can have a devastating impact in all the system. This study was made by computational fluid dynamics (CFD) and finite element analysis (FEA). Pressure, stress and safety factor about three blades with different profiles (Eppler E817, NREL S802 y NACA 4412) were evaluated. Three different materials were used for each blade (stainless steel, aluminium and low-density polyethylene). The studied materials can be selected to build the blades due to their stiffness, hydrodynamic strength, corrosion, erosion resistance and low weight, being the aluminium the one that presents the best balance of desirable properties.

Keywords: Hydrokinetic Turbine, Finite Element Analysis, Computational Fluid Dynamic)

I. INTRODUCTION

The combination of THK and diesel generators is the best option to supply electrical energy in small populations of rural areas far from large generation centers [1] [2] .Numerical and experimental investigations have been carried out to evaluate and improve the performance of different THK rotors [3][4]. To achieve this, different hydrodynamic profiles have been used on which the efficiency in the conversion of hydraulic to mechanical energy that occurs through the rotor depends [4]. However, the evaluated turbines have a maximum power coefficient – Cp for Tip Speed Ratios -TSR with its acronym in English, used in each study, when the profile or the TSR change, the efficiency changes too.

The main requirements of THK blades are low weight, strength, and corrosion resistance. Their efficiency and performance depend on the hydrodynamic profile. However, from the point of view of structural strength, the thickness of the blade cross sections near to the blade root should be increased. In general, the design thickness of the blade sections also depends on the length of the span and the hydrodynamic requirements. On the other hand, the strength and reliability of the blades of the hydrokinetic turbine depend on the properties of the material used for their manufacture and their behavior under load [5][6].

Davies and others, performed static and cyclic tests in air and seawater, quantifying the influence of aging in seawater on fatigue performance, and measured shorter fatigue lives after aging [7]. Singh and Choi carried out a pressure, stress, and deformation study about two different blades, one of them with shorter chord length in contrast to the typical blade for sea current turbines. For the study used two different materials for each blade: aluminium and steel, finding that the stress and the deformation were three times greater for the typical blade, regardless of the material with which it was built [8]. Muñoz and other, propose a software design tool and manufacturing methods of low cost within the reach and understanding of less developed communities, using classical materials mechanics for the preliminary structural verification [9]. Troncoso affirmed that the Blade Element Momentum (BEM) demonstrated versatility by allowing rapid modification and evaluation of rotor blades and thus, was possible to determine the applied forces over each section of the blade, which were employed in the FEA for the structural analysis [10].

Chica and others report the structural design of the THK blades in composite materials combining blade element momentum (BEM) to predict the hydrodynamic performance, and CFD to evaluate it, with a water velocity of 1.5 m/s, TSR of 6.325, attack angle of 5° and pitch angle of 0°, using a S822 profile. The power coefficient obtained was 0.4382, and the fluid domain was coupled to the structural domain through a one-way coupling, the FEA analysis of structure interaction with fluid was carried out to discover the blade geometry effect and the operation conditions on the developed stresses [11]. Wang and others employed ANSYS Fluent® to calculate the hydrodynamic loads and Ansys Static Structural® to determine the structural response. The CFD and FEA interface was based on a unidirectional coupling, in which the hydrodynamic loads calculated from the CFD modelling were assigned to the FEA

modelling as load boundary conditions. The maximum tension and compression stresses and the deformations of the tip in each case were within limits of the materials in accordance with relevant design standards [12]. Payne, Stallard and Martinez employed FEA to get the stresses and deformations on the Blade, obtaining errors less than 6% for the experimental deflection [13].

For this reason, has been necessary to evaluate numerical and experimentally the efficiency of the THK rotors of horizontal axis with different hydrodynamic profiles. In this study were evaluated with a flow rate of 1.4 m/s. This is the characteristic velocity of South American hydrography. The application in picogeneration in this region in need that has a big potential. Three THK rotors were designed through mathematical modelling BEM, using the hydrodynamic profiles NACA 4412, NREL S802, y EPPLER 817, it was simulated their hydrodynamic behavior using CFD techniques in the ANSYS CFX® software, to verify the power coefficient (Cp) predicted during the design BEM with different TSR. Finally, it was used the pressure profile on each blade to evaluate structurally the blades, through FEA in ANSYS Static Structural®, to determine their safety factor.

II.   METHODOLOGY

A.   ROTOR DESIGN

ITM test bench spatial dimensions were considered. That allows a turbine radius equal to 0.25m, and a fluid density (ρ) at 20°C equal to 998.29 kg/m3. With a flow rate (U) of 1.4 m/s, typical of the Colombian rivers [14], the Reynolds (Re) was calculated with the initial supposition of a chord length (c) equal to 25 mm (R/10). Water kinematic viscosity (v) at 20°C of 9.79 m2/s and the flow rate on the blade is considered as the relative velocity (w) between the turbine rotation and the flow rate (U), w varies between 5 and 6 m/s. Value of Reynolds in the blade surface, since the leading edge and trailing edge, equal to 300.000. Were founded three recommended families of profiles in the literature because their performance in aquatic applications [15][16][17], NACA 44XX, Eppler E8XX y NREL S8XX. The values of Reynolds obtained are entered in the XFOIL® MIT software varying the attack angle (α) of each profile from -10° to 30° with steps of 0.001°, to find the inclination with maximum fineness (ratio between the lift coefficient and the drag coefficient – CL/CD) and were selected NACA 4412, E817 and S835. From the selected profiles were obtained the intrados and extrados in airfoiltools® and were exported to the ANSYS DesignModeler®.

Using the BEM theory were determined the geometries with better performance for the TSR from 1 to 6, the most common for THK [18][19][20] , considering that for water low velocities the optimal number of blades (Nb) is three [21] and the number of sections (n) in which the blade was divided for calculation purposes was 10. The BEM methodology consists in the creation of blades for a rotor with a radius "r", dividing them by sections (n) and calculating, section by section, the different parameters that give the shape. The values of torque and power calculated keeping this procedure are the maximum for each TSR, obtaining that the best performance was between 3.5 and 3.6. For the three hydroprofiles, were selected the maximum Cp of each curve to obtain the TSR that gives the best performance, in consequence the values of chord and torsion angle associated are collected and used to model the three rotors, through Design Modeler®. The torsion angles and the chord of the profiles NACA 4412 and NREL S802 are similar, but as the thickness and shape of both profiles is different, the rotors performance change. The Eppler profile has differences in the bank angle of 2° approximately in all the sections and of 0.01 m respect to the chord making the blades of this rotor larger.

In Design Modeler®, with the pattern tool, were replicated 10 equal profiles in the Z axis with a separation between the profiles gives by the division between the rotor radius and the number of sections (n). Using the value of the chord, calculated by BEM for each profile, are scaled in X and Y axis. Depending of the section and then each one is rotated according to the calculated torsion angle, obtaining as result the framework; after that, were covered the curves created with the skin operation, of this way, was obtained the solid blade, using the pattern tool were created two blades more and were ubicated at 120° and 240°. Then the hub design was complemented, which is the same for the three rotors and its dimensions are a cylinder of 0.12 m of diameter and a total length of 0.10 m generated by an extrusion. With the same diameter was create a semi sphere at the top. The blades and hub are brought together to finally create the rotor. Figure 1 shows the blade design result with the Eppler E817 hydrofoil.

Then Boolean operations were used to create two different fluids. The first fluid is rotating and has the rotor, it is built with a circle with a radius of 0.45 m [22] and it also has a height of 0.65 m. The second fluid is stationary and has the previous fluid. This enters freely in the opposite direction to the axis. This control volume has a total length of 2,775 m and a radius of 1.25 m [23]. As it is a symmetric geometry that is repeated three times, a third of the total volume is simulated to save computation time, this simplification does not affect the results [24] [25]. After defining the geometry and the control volumes, the extraction of the turbine geometry was carried out on the first fluid, and then the subtraction of the first fluid was carried out on the second, thus leaving only two control volumes. This entire procedure was performed for all three rotors.
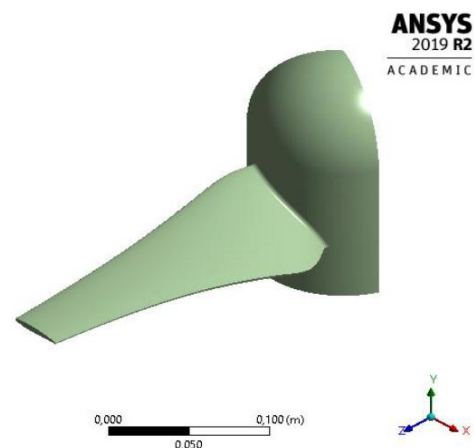

Fig. 1.   Blade and hub with Eppler E817 hydrofoil.

B. CFD simulation

The template is used to format your paper and style the text. All margins, column widths, line spaces, and text fonts are prescribed; please do not alter them. You may note peculiarities. For example, the head margin in this template measures proportionately more than is customary. This measurement and others are deliberate, using specifications that anticipate your paper as one part of the entire proceedings, and not as an independent document. Please do not revise any of the current designations.

When the rotor models were obtained, the control volumes of the external fluid and the fluid around the rotor were discretized. Mesh was performed on the ANSYS Meshing® module, using the proximity and curvature function to densify the region surrounding the blade and rotor. This is the area where the phenomenology of interest occurs. Then the element size was decreased to have a minimum value of 8 mm per element. This increased the number of elements to 1,000,000. The metrics of the generated mesh were evaluated. The maximum values for the orthogonal quality were 0.7 and the minimum skewness was 0.3. Both values are in the range of acceptability of the software manual. This was the first mesh, but not the definitive one, since a mesh independence study was performed later. Meshing was done on an HP Z600 Workstation with a 2.66 GHz processor and 48 GB of RAM using 12 processing cores.

Symmetry interfaces were defined on the flat faces of the control volume to indicate the phenomenology is repeated in the next section. The boundaries were configured with a velocity in the normal direction at the inlet of 1.4 m / s. The output is configured as free discharge at atmospheric pressure. Between the two previous volumes, the non-slip wall condition and periodic rotational condition are configured in the symmetry interface. The simulation was configured as transient with 4 seconds with an adaptive time step ranging from 0.01s to 0.00001s. This time step was established by means of the courant number equation, for this the smallest size of the mesh element and the velocity of the fluid on the blade surface were used, which is the point where these mesh elements are presented. The outer domain is considered stationary and the fluid surrounding the rotor is configured as rotary. The change of frame was configured as "Frozen rotor" and the interface model was general connection. For periodic interfaces the interface model was rotational periodic. After completing the configuration, the torque on the blade surface was selected as the monitoring variable. For the simulations, a DELL T7600 Workstation with a 2.9 GHz processor, 32 GB of RAM was used and 12 cores were used in parallel for the double precision solution.

When is obtained the first stable torque result, it was parameterized to continue with the mesh independence study. For mesh independence studies, tetrahedral meshes from 300,000 to 30,000,000 elements were created. A mesh is independent when the torque variation is less than 3% when compared to the denser mesh (relative error). With the selected meshes, the study of Cp against TSR was parameterized, always selecting the same mesh and varying only the angular velocity from 0.1 rad / s to 40 rad / s.

With this study, pressure profiles were obtained for each of the rotors. These profiles are presented in Figure 2, by way of example, for the NACA 4412 hydroprofile rotor on the extrados (upper region) and on the intrados (lower region) for TSR 1 and 3.55. The latter is the maximum Cp predicted by the BEM methodology, colored according to the pressure exerted by the fluid on Pascal's (Pa) as a result of the hydrodynamic interaction. The contours show the distribution of the load on the blade. There are two evidence things: 1. When increase the angular velocity and getting closer to the maximum Cp, where the best efficiency of the turbine is presented, you increase the loads. It is evident that the maximum pressures in TSR 1 are 2.0 kPa and -5.4 kPa, while in TSR 3.55 they increase appreciably to 19.8 kPa and -60.9 kPa. 2. Both scenarios show that the highest hydrodynamic load is experienced at the leading edge.
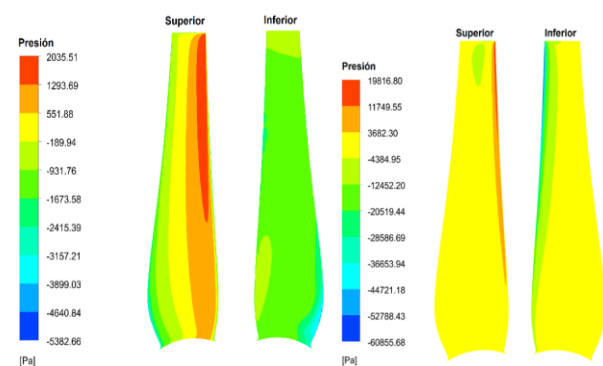
Fig. 2. Pressure contours on the blade with NACA 4412 profile seen from the top and bottom for TSR 1 (a) and TSR 3.55 (b).
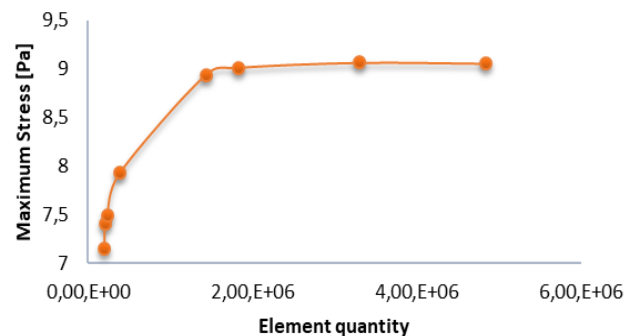*(Own source.)*

Figure 3 shows the behavior of the pressure around different sections of the blade by means of contours for TSR 1 and 3.55. For TSR 1, it can be seen that the highest pressures are concentrated in the upper part of the profile in all the sections of the blade since in this area the fluid hits. Low pressures are present on the intrados of all sections, this is due to the angle at which the fluid hits the blade. This causes low lift coefficient in the blade, this generates low performance and makes the torque of the turbine low. For TSR 3.55 a similar behavior is observed, but with less intensity. High pressure contours are observed at the leading edge of all sections and do not extend over much of the top. This is because the relative angle between the fluid and the profile approaches the optimal angle of attack. This makes the pressure gradient between the

extrados and the intrados is negative. When this phenomenon occurs, the intrados pressures make the lift forces higher, directly increasing the torque. This phenomenon indicates that the TSR that maximizes the Cp is close to this value.
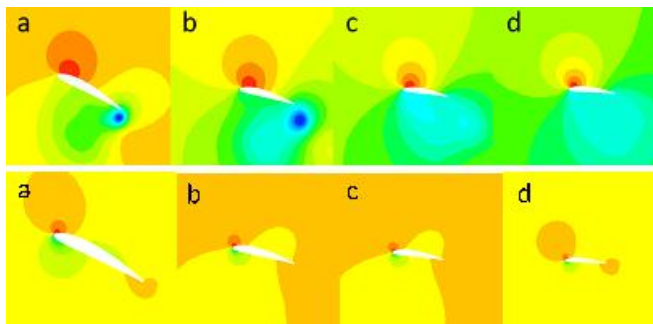
Fig. 3. Pressure profiles for TSR 1 (top) and TSR 3.55 (bottom) on rotor blade with NACA 4412 profile in different sections a) 30% b) 50% c) 70% d) 90% of radius.
(Own source.)

III. RESULTS AND DISCUSSION

A. FEA STUDY

The structural analysis was done after the hydrodynamic design and the determination of the external loads through CFD as was detailed in the previous section. In that section, was studied the flow around the THK blades to detect the hydrodynamic loads of the extrados and intrados surfaces and of the leading edge that the blade will find in extreme flow conditions (maximum Cp). The loads were imported to the ANSYS Static Structural®. There was located the centrifugal load in the rotation center of the rotor and the gravity was defined. The fluid-structure interaction system was created to perform static analysis through the use of pressure loads (hydrodynamic loads) in the blade from CFD to transfer them through a mapping alghorithm and project them on the blade surface with a global coordinate system. The solution of the pressure loads on the blade obtained from CFD was connected to the FEA module configuration and these loads were used as mechanical loads (boundary conditions) for the static analysis of the blade.

The geometries were modeled in DesignModeler® as was detailed previously. As can be observed in the Figure 1, this segment begins in a hub with a radius that pretends decrease the stress concentration in the embedment. In this location the highest flexural loads are expected. The stress concentration was previously studied by the authors in different geometries of machine elements [26]. When the geometry was complete in Design Modeler® was transferred to Static Structural® (Ansys Workbench). There was meshed with the appropriate element type. The unstructured tetrahedral mesh of the solid blades for the models converged rapidly with 205.650 elements for the E817, with 357.720 elements for the NACA 4412 and with 493.690 for the S802. All of them with an element size of 15 mm. The independence of the results was evaluated reducing the element size until 0.45 mm. With this last size were generated 4'833500 elements. 8 meshes were evaluated, checking the maximum stress. In the figure 4 can be observed the results of the evaluation of the blade with the E817 profile.

The independence was achieved from the element size equal to 1 mm with meshes of 1'434.300 elements. The relative errors were below to 2%. The checked variable is independent of the material.

Fig. 4. Independence of the mesh. E817 hydroprofile.
(Own source.)

In the preprocessing mode, all the parameters can be created and assigned to the geometry (FE mesh). These parameters are transferred to the FE model and to the solver input file. In postporcessing mode, after a complete solution and the importation of the result files, the results can be viewed and evaluated, stresses, deformations and safety factor.

The high flexural moments detected during the operation, require materials with high specific resistance and stiffness for the blade maintains its shape under high loads. As the blade can be submerged for long periods of time in hard water, maybe corrosive, can be cause the degradation of certain properties of the material. The manufacture and costs must be considered. Thus, the material used must resist corrosive environments and erosive wear and, at the same time, keeps high levels of strength and stiffness. Many authors have suggested a wide range of materials as glass fiber, carbon fiber, reinforcement polymers, woods, metals, and others. To evaluate the viability of different materials for the manufacture of the blades were created some static numerical models for each geometry using the materials with physical and mechanical properties are important for the present study (Table 1)

When the kind of materials were defined in the Workbench project, the loads were imported from CFX® and the boundary conditions and the specific analysis options were applied to the model. Finally, the analysis was run. Three hydrodynamic profiles and three materials were investigated to know the mechanical behavior of the blade in aspects as geometry, tip deviation and stress levels developed by the external loads. All blade models were considered as a cantilever beam with all degrees of freedom fixed in the hub. Centrifugal, gravitational and hydrodynamic loads were used for the structural analysis. The Von Mises stresses and the deformations for the combinations of profiles and materials.

As was expected, the magnitude of the developed stresses in the solid was quasi-independent of the material of the blade but dependent of the geometry and the loads. In the Figure 5 can be observed the contours that describe the Von Mises stress

distribution due to the combination of the internal loads in the material. In this case, for the THK blade with the E817 hydroprofile. It is observed that the magnitude of the efforts is located in the critical position that is located at the base of the profile that is relieved by the radius of agreement made in the design. For the more robust hydroprofile (E817) the Von Mises stresses reached a critical value of 9.0724 MPa as shown in the Figure. For the NACA 4412 and NREL S802 hydroprofiles, which are slimmer and lighter designs, the maximum Von Mises stresses reached values of 14.35 and 12,766 MPa, respectively.

It was evident the influence of the geometry and the material in the blades behavior. In the Figure 6 are compared the deformations developed in the blades with the E817 hydroprofile. This one is the most robust, therefore, presented less deformation with each kind of material. In the same Figure are showed the two blades that obtained the extreme results. The lowest deformation was equal to 0.35 mm with stainless steel. The highest deformation achieved 11.042 mm with the polyethylene. The above fulfils with the mechanical properties of the studied materials. It was expected too that the maximum displacement occur in the cantilever beam free end.

Table 1. Main physical and mechanical properties of the materials evaluated. Source: Ansys.

	Stainless steel	Aluminium	Low density polyethylene
Density [kg/m3]	7750	2710	924
Young's modulus [Pa]	1.93x1011	7.05x1010	2.21x108
Poisson ratio	0.31	0.33	0.448
Shear modulus [Pa]	7.3664x1010	2.6504x1010	7.6312x107
Yield stress [Pa]	2.07x108	3.49x107	1.14x107
Ultimate strength [Pa]	5.86x108	7.99x107	1.87x107

The previous results are focused in the last evaluation related with the safety factor, which depends on the properties of the materials studied and how they react under the loads according to the geometry of each blade. In this evaluation was verified that all kind of materials and profiles are viable for the technological development of THK. The stainless steel is oversized for the application and the low-density polyethylene, for slender profiles, near to the below safety limit but in the fulfil range. The minimum safety factor in the highest position of the range was equal to 6.5 for the E817 profile (the most robust profile), simulated with the high strength material: stainless steel. This safety factor corresponds to the location where the stress is maximum: the root of the blade in the hub. The minimum safety factor in the lowest position of the range corresponds to the NACA 4412 profile (the most slender profile) with the less strength material: low density polyethylene.
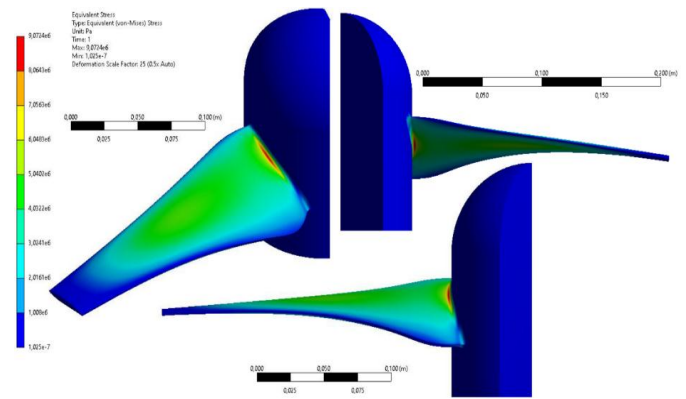
Fig. 5. Independence of the mesh. E817 hydroprofile.
(Own source)
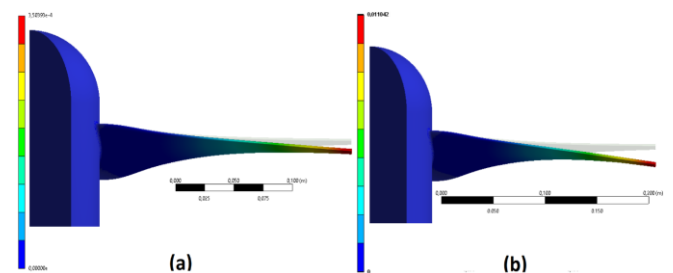
Fig. 6. Deformation contours on the blade. E817 hydroprofile. (a) Stainless steel, (b) low density polyethylene.
(Own source)

IV. CONCLUSION

Nine THK blades were evaluated with hydrodinamic profiles: EPPLER E817, NREL S802 and NACA 4412, studying through CFD the flow around each rotor to determine the hydrodinamic loads on the blades and importing these loads in FEA to perform the study of the mechanical behaviour with three different materials: stainless steel and low density polyethylene.

For the flow conditions simulated, the NACA 4412 and NREL S802 profiles (more slender) developed maximum stresses equal to 14.35 and 12.766 MPa respectively. By other way, the E817 Eppler achieved 9.0724 MPa. For this reason the minimum safety factors found in the root of the blade with the NACA profile and manufactured in polyethylene are equal to 1.2 and manufactured in aluminium equal to 3.8. The blade with Eppler profile manufactured in stainless steel reported values of minimum safety factor of until 6.5.

FEA indicated that the THK blade geometries would satisfactorily withstand the force exerted on it under the combined effects of the centrifugal, gravitational and hydrodynamic loads studied since for the external loads analyzed in the blade it is possible to verify that the Von Mises Stresses are under the elastic limit of the applied materials, avoiding that the blades fails. The maximum deflection observed of all modelled blades was located in the tip of the profile. The minimum deflection was located in the root of the

profile. The Von Mises stresses were higher in the root and decreasing towards the tip in the leading edge of the blades.

The materials studied can be selected to the manufacture of the blades because their stiffness, hydrodinamic strength, corrosion and erosion strength and low weight. The aluminium presents the best balance in desirable properties. It is necessary the technic and economic evaluation that considers the unit cost of the material, the costs associated to the manufacture according to the applied processes, achieving a minimum profitable production and the evaluation of the useful life to do a projection that considers maintenance costs.

REFERENCES

[1] M. Anyi and B. Kirke, "Energy for Sustainable Development Tests on a non-clogging hydrokinetic turbine," *Energy Sustain. Dev.*, vol. 25, pp. 50–55, 2015.

[2] H. J. Vermaak, K. Kusakana, and S. P. Koko, "Status of micro-hydrokinetic river technology in rural applications: A review of literature," *Renew. Sustain. Energy Rev.*, vol. 29, pp. 625–633, 2014.

[3] J. N. Goundar and M. R. Ahmed, "Design of a horizontal axis tidal current turbine," *Appl. Energy*, vol. 111, pp. 161–174, 2013.

[4] W. Q. Wang, R. Yin, and Y. Yan, "Design and prediction hydrodynamic performance of horizontal axis micro-hydrokinetic river turbine," *Renew. Energy*, vol. 133, pp. 91–102, 2019.

[5] C. J. Bai, F. B. Hsiao, M. H. Li, G. Y. Huang, and Y. J. Chen, "Design of 10 kW horizontal-axis wind turbine (HAWT) blade and aerodynamic investigation using numerical simulation," *Procedia Eng.*, vol. 67, pp. 279–287, 2013.

[6] D. M. Grogan, S. B. Leen, C. R. Kennedy, and C. M. Ó Brádaigh, "Design of composite tidal turbine blades," *Renew. Energy*, vol. 57, pp. 151–162, 2013.

[7] B. Gaurier, P. Davies, A. Deuff, and G. Germain, "Flume tank characterization of marine current turbine blade behaviour under current and wave loading," *Renew. Energy*, vol. 59, pp. 1–12, 2013.

[8] P. M. Singh and Y. Do Choi, "Shape design and numerical analysis on a 1MW tidal current turbine for the south-western coast of Korea," *Renew. Energy*, vol. 68, pp. 485–493, 2014.

[9] A. H. Muñoz, L. E. Chiang, and E. A. De la Jara, "A design tool and fabrication guidelines for small low cost horizontal axis hydrokinetic turbines," *Energy Sustain. Dev.*, vol. 22, no. 1, pp. 21–33, 2014.

[10] C. Troncoso, "Diseño de un rotor hidrocinético usando perfiles NACA y NREL," 2014.

[11] J. Aguilar, A. Rubio-Clemente, and E. Chica, "Fluid-structure interaction of a hydrokinetic turbine," *MECÁNICA Mater. IV Exp. Model. NUMÉRICO Y TEÓRICO*, vol. 53, no. 9, pp. 45–56, 2016.

[12] L. Wang, R. Quant, and A. Kolios, "Fluid structure interaction modelling of horizontal-axis wind turbine blades based on CFD and FEA," *J. Wind Eng. Ind. Aerodyn.*, vol. 158, pp. 11–25, 2016.

[13] G. S. Payne, T. Stallard, and R. Martinez, "Design and manufacture of a bed supported tidal turbine model for blade and shaft load measurement in turbulent flow and waves," *Renew. Energy*, vol. 107, pp. 312–326, 2017.

[14] IDEAM, "IDEAM-Instituto de Hidrología, Meteorología y Estudios Ambientales.," 2014. [Online]. Available: http://www.ideam.gov.co/.

[15] E. Koç *et al.*, "Numerical and experimental analysis of the twin-blade hydrofoil for hydro and wind turbine applications," *Ocean Eng.*, vol. 97, pp. 12–20, 2015.

[16] N. Kaufmann, T. H. Carolus, and R. Starzmann, "An enhanced and validated performance and cavitation prediction model for horizontal axis tidal turbines," *Int. J. Mar. Energy*, vol. 19, pp. 145–163, 2017.

[17] J. D. Betancur, J. G. Ardila, A. Ruiz, and E. L. Chica, "AERODYNAMIC PROFILES FOR APPLICATIONS IN HORIZONTAL AXIS HYDROKINETIC TURBINES," vol. 10, no. 03, pp. 1962–1973, 2019.

[18] P. Mycek, B. Gaurier, G. Germain, G. Pinon, and E. Rivoalen, "Numerical and experimental study of the interaction between two marine current turbines," *Int. J. Mar. Energy*, vol. 1, pp. 70–83, 2013.

[19] P. Mycek, B. Gaurier, G. Germain, G. Pinon, and E. Rivoalen, "Experimental study of the turbulence intensity effects on marine current turbines behaviour. Part I: One single turbine," *Renew. Energy*, vol. 66, pp. 729–746, 2014.

[20] J. D. Betancur, J. G. Ardila Marin, and E. L. Chica Arrieta, "Design and hydrodynamic analysis of horizontal-axis hydrokinetic turbines with three different hydrofoils by CFD," *J. Appl. Eng. Sci.*, pp. 1–8, 2020.

[21] J. Seo, J.-H. Yi, J.-S. Park, and K.-S. Lee, "Review of tidal characteristics of Uldolmok Strait and optimal design of blade shape for horizontal axis tidal current turbines," *Renew. Sustain. Energy Rev.*, 2019.

[22] P. Jeffcoate, T. Whittaker, C. Boake, and B. Elsaesser, "Field tests of multiple 1/10 scale tidal turbines in steady flows," *Renew. Energy*, vol. 87, pp. 240–252, 2016.

[23] S. J. Kim, P. M. Singh, B. S. Hyun, Y. H. Lee, and Y. Do Choi, "A study on the floating bridge type horizontal axis tidal current turbine for energy independent islands in Korea," *Renew. Energy*, vol. 112, pp. 35–43, 2017.

[24] J. H. Lee, S. Park, D. H. Kim, S. H. Rhee, and M. C. Kim, "Computational methods for performance analysis of horizontal axis tidal stream turbines," *Appl. Energy*, vol. 98, pp. 512–523, 2012.

[25] H. Yang, W. Shen, H. Xu, Z. Hong, and C. Liu, "Prediction of the wind turbine performance by using BEM with airfoil data extracted from CFD," *Renew. Energy*, vol. 70, pp. 107–115, 2014.

[26] F. Hoyos G, J. D. Betancur G, D. Osorio P, and J. G. Ardila M, "Construcción de curvas de factor de concentración de esfuerzos por medio de simulaciones.," vol. 21, no. 75, pp. 35–43, 2016..